



ELSEVIER

Available online at [www.sciencedirect.com](http://www.sciencedirect.com)

SCIENCE @ DIRECT®

Physics Letters A 330 (2004) 481–486

PHYSICS LETTERS A

[www.elsevier.com/locate/pla](http://www.elsevier.com/locate/pla)

# Longitudinal momentum mining of beam particles in a storage ring

C.M. Bhat

*Fermi National Accelerator Laboratory, P.O. Box 500, Batavia, IL 60510, USA*

Received 3 August 2004; accepted 18 August 2004

Communicated by F. Porcelli

---

## Abstract

I describe a scheme for selectively isolating high density low longitudinal emittance beam particles in a storage ring from the rest of the beam without emittance dilution. I discuss the general principle of the method, called longitudinal momentum mining, beam dynamics simulations and results of beam experiments. Multi-particle beam dynamics simulations applied to the Fermilab 8 GeV Recycler (a storage ring) convincingly validate the concepts and feasibility of the method, which I have demonstrated with beam experiments in the Recycler. The method presented here is the first of its kind.

© 2004 Elsevier B.V. All rights reserved.

PACS: 29.27.Bd; 29.20.Dh; 29.29.-c

Keywords: Beam emittance; Storage rings; Longitudinal beam dynamics; Momentum mining; Antiproton beam

---

## 1. Introduction

One of the most important problems encountered in high-energy hadron beam storage rings is to select only the high intensity, low emittance, region of the *phase space* of beam particles with minimal emittance dilution. Considerable progress has been made over the years on techniques for doing this, broadly referred to as momentum mining [1,2]. Typically, the region of interest in the beam particle distribution lies in the vicinity of the *synchronous* particle [3]. Antiproton storage rings both at CERN [4] and at Fermilab [5]

have adopted what I call transverse momentum mining for extracting the dense beam from a stack of cooled beam particles. For example, in the antiproton Accumulator Ring at Fermilab, a part of the stored beam is captured adiabatically in *buckets* of sinusoidal radio-frequency (rf) waves with *harmonic number*  $h = 4$  and *bucket area* smaller than the total beam phase space area. Subsequently, the beam particles in  $h = 4$  buckets are pulled out radially from the main stack through acceleration. Once completely outside the main stack, the particles are extracted. The shortcoming of this method is the inevitable beam disruption caused by the acceleration of the low emittance beam particles through the main stack. This leads to longitudinal emittance growth of the beam left in the main stack.

---

*E-mail address:* [cbhat@fnal.gov](mailto:cbhat@fnal.gov) (C.M. Bhat).

Furthermore, if the beam extraction is carried out multiple times, the bunches in the later extractions suffer from lower particle densities and higher longitudinal emittance. The overall longitudinal emittance growth in the Accumulator Ring is found to be nearly 300% during the entire extraction process. This leads to degraded proton–antiproton luminosity in the Tevatron [5].

Another method for proton mining using dual frequency amplitude modulation has been proposed [6, 7], which is very similar to the transverse mining method.

In this Letter, I propose a new technique [8] for mining beam particles from the high density region of the *longitudinal* phase space with minimal emittance dilution. This novel technique depends crucially on the existence of *barrier rf* technology (which was introduced in 1983) [9] and the mining illustrated here is done using rectangular barrier rf buckets.

## 2. The principle of longitudinal momentum mining

A particle beam in a storage ring is characterized by its energy spread  $\Delta\hat{E}$  about its synchronous energy  $E_0$  and a characteristic transverse emittance. In the absence of *synchro-betatron coupling* these two quantities can be varied independently of each other. Generally, the energy distribution of the particles in the storage ring is approximately parabolic or Gaussian in shape with the synchronous particles at the peak. The Hamiltonian of any particle with energy  $\Delta E$  relative to the synchronous particle in a *synchrotron* is given by [10,11]

$$H(\tau, \Delta E) = -\frac{\eta}{2\beta^2 E_0} \Delta E^2 - \frac{e}{T_0} \int_0^\tau V(t) dt, \quad (1)$$

where  $\eta$ ,  $T_0$  and  $\beta$  are the phase slip factor, the revolution period and the ratio of the particle velocity to that of light, respectively, and  $-\tau$  is the time difference between the arrival of this particle and that of a synchronous particle at the center of the rf bucket.  $V(t)$  is the amplitude of the rf voltage wave-form. We identify the second term of the above equation as the

potential energy  $U(\tau)$  of the particles, given by

$$U(\tau) = -\frac{e}{T_0} \int_0^\tau V(t) dt. \quad (2)$$

For a rectangular barrier bucket,  $V(t)$  is given by

$$V(t) = \begin{cases} -V_0 & \text{for } -T_1 - T_2/2 \leq t < -T_2/2, \\ 0 & \text{for } -T_2/2 \leq t < T_2/2, \\ V_0 & \text{for } T_2/2 \leq t < T_1 + T_2/2, \end{cases} \quad (3)$$

where  $T_1$  and  $T_2$  denote barrier pulse width and gap between rf pulses as shown in Fig. 1. A schematic view of the rf wave form with the beam phase space boundary (dashed line in left figure) and the corresponding potential well, containing beam particles for a storage ring operating below *transition energy* is shown in Fig. 1(a).

The objective of longitudinal momentum mining is to isolate particles closer to  $E_0$  from the rest. This is accomplished by adiabatically inserting a mining bucket inside the existing well (between  $-T_2/2$  and  $T_2/2$ ), as indicated by arrows in Fig. 1(b) (left), so that all particles with energy near the synchronous energy, including synchronous particles, drift to the lowest potential. It is important to note that the trapping of particles takes place during the adiabatic opening of the mining bucket. Since the synchrotron oscillation periods of the particles with energy closest to  $E_0$  are very large, the drift times are very long. Therefore, to expedite the mining process, and to ensure the trapping of particles with energy  $E_0$ , one can grow a negative pulse immediately to the right of the left-most rf pulse (at  $-T_2/2$ ) and shovel particles adiabatically to a location to the right indicated by  $T_a$ . The final voltage wave form for this configuration is given by

$$V(t) = \begin{cases} -V_0 & \text{for } -T_1 - T_2/2 \leq t < -T_2/2, \\ 0 & \text{for } -T_2/2 \leq t < T_a, \\ -V_1 & \text{for } T_a \leq t < T_b, \\ 0 & \text{for } T_b \leq t < T_c, \\ V_1 & \text{for } T_c \leq t < T_2/2, \\ V_0 & \text{for } T_2/2 \leq t < T_1 + T_2/2. \end{cases} \quad (4)$$

The longitudinal emittance of the trapped particles in the mining bucket between  $T_a \leq t < T_2/2$  is given by  $\varepsilon_m = 2(T_c - T_b)\Delta E_m + 4T_0|\eta|\Delta E_m^3/(3\beta^2 E_0 e V_1)$  where  $\Delta E_m = \sqrt{2\beta^2 e V_1 (T_b - T_a) E_0 / (T_0 |\eta|)}$  and  $e$  is

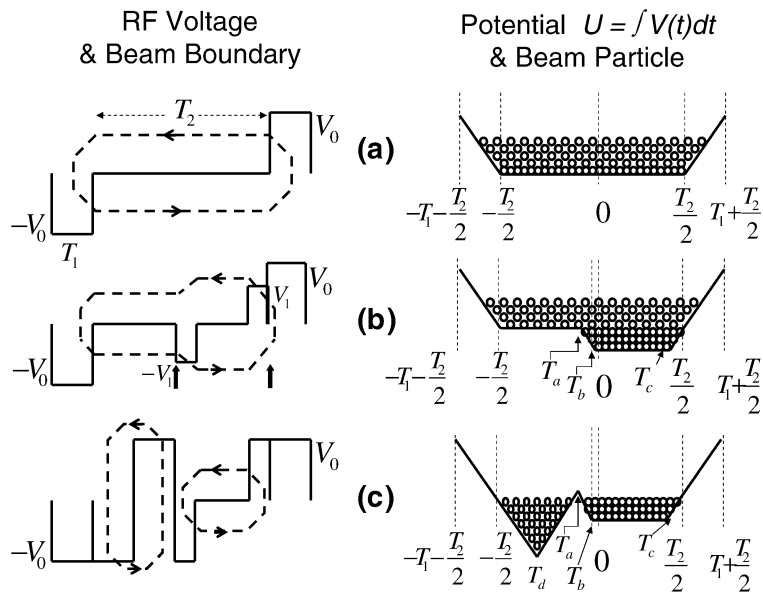


Fig. 1. Schematic view of longitudinal momentum mining using barrier buckets. Barrier rf voltage (solid lines) and beam particle boundary in  $(\Delta E, \tau)$ -phase space (dashed line) are shown on the left. The cartoons on the right show potential well and the beam particles in it. (a) The initial distribution, (b) after confining particles with low energy spread in a deeper well and (c) after isolating particles with high and low energy spreads.

the electron charge. Finally, to isolate the remaining particles from those that are trapped, another rf bucket is opened in the region  $-T_2/2 \leq t < T_a$  as shown in Fig. 1(c). Thus are the particles with low longitudinal emittance mined while leaving the rest in the region  $-T_2/2 \leq t < T_a$ .

One can think of numerous variations of the method described above. For example, one can start with a cooled beam in a barrier bucket of pulse gap of  $T_2/2 - T_a$  instead of  $T_2$ , change the order of the rf manipulation sequences so that the particles near synchronous energy are never disturbed and still reach the stage illustrated in Fig. 1(c).

### 3. Application to the Fermilab Recycler

We have applied the scheme described above to the beam in the Fermilab Recycler [12]. The Recycler is an 8 GeV synchrotron storage ring that operates below the transition energy ( $\gamma_T = 21.6$ ) and has  $T_0 = 11.12 \mu\text{s}$ . This will be the main antiproton source for the proton–antiproton collider program at Fermilab. The antiproton beam is stacked and stored

azimuthally in the Recycler using barrier buckets generated by a broad-band rf system [13] capable of providing rf pulses of 2 kV. The beam is cooled initially using stochastic cooling [14] and is expected to be cooled further with electron cooling [15] to  $\leq 54 \text{ eV s}$  longitudinally and  $\leq 7\pi \text{ mm mrad}$  transversely. We plan to accumulate  $> 6 \times 10^{12}$  antiprotons [16] in the Recycler before they are transferred to the Tevatron. Either a part of the cooled beam or the entire stack will be extracted in nine transfers of equal emittance and equal intensities, each with four 2.5 MHz bunches. Thus, there will be thirty six antiproton bunches in the Tevatron from the Recycler. The longitudinal emittance of each bunch at the time of extraction is expected to be  $\leq 1.5 \text{ eV s}$ . Stacking and unstacking of antiprotons from the Recycler entails complicated sets of rf manipulations [17]. In order to achieve high proton–antiproton *luminosity* in the Tevatron, it is essential to maintain the emittance of the beam throughout the chain of rf manipulations in the Recycler and to send only a high density low longitudinal emittance beam to the Tevatron.

Our testing of the method of longitudinal momentum mining in the Recycler was carried out in

two steps. First, computer simulations using a multi-particle beam dynamics code, ESME [18], were carried out to establish the mining steps. Then, experiments were done with beam in the Recycler to demonstrate the technique.

### 3.1. Beam dynamics simulations

The simulation results presented here assume about 100 eV s of beam in the Recycler captured in a rectangular barrier bucket. The primary goal was to mine 54 eV s of the low longitudinal emittance high density part of the phase space distribution of the beam and capture the rest of the beam in a separate bucket.

Fig. 2 shows the beam particle distribution in  $(\Delta E, \tau)$ -phase space for different stages of mining. The beam distributions before and during mining are shown in Fig. 2(a) (energy spread of  $\pm 5.7$  MeV) and (b), respectively. The width and amplitude of the barrier pulses used were, respectively,  $0.9 \mu\text{s}$  and 2 kV for the initial distribution (Fig. 2(a)). Fig. 2(b) shows the distribution after populating all of the low emittance particles to the right-hand side in a mining bucket (indicated between two arrows). The size of the mining bucket was chosen to be 54 eV s with rf pulse amplitude of 0.27 kV, width of  $0.34 \mu\text{s}$  and a pulse gap of  $6.13 \mu\text{s}$ . All particles with energy spread less than the bucket-height of the mining bucket are confined to the right-hand side while the rest move freely throughout the original bucket. (These two cases correspond to the schematic picture shown in Fig. 1(a) and (b).)

The isolation of 54 eV s low emittance high density beam was accomplished by opening a bucket (indicated by an arrow in Fig. 2(c)) of an area  $\geq 46$  eV s; the area and height of this bucket was chosen to be 74 eV s and  $\pm 21.7$  MeV, respectively. Fig. 2(c) shows the final phase space distribution after completion of mining. The total phase-space area was found to be preserved to better than 10% at the end of all rf manipulations. All of the emittance growth was seen in the 74 eV s bucket and occurred during the opening of this bucket.

Finally, the 54 eV s beam was divided into nine bunches of equal intensity and equal longitudinal emittance simply by adiabatic capture (e.g., see Fig. 3(b)) and, each of the nine bunches were further divided into four 2.5 MHz bunches each with 1.5 eV s and were prepared for collider operation.

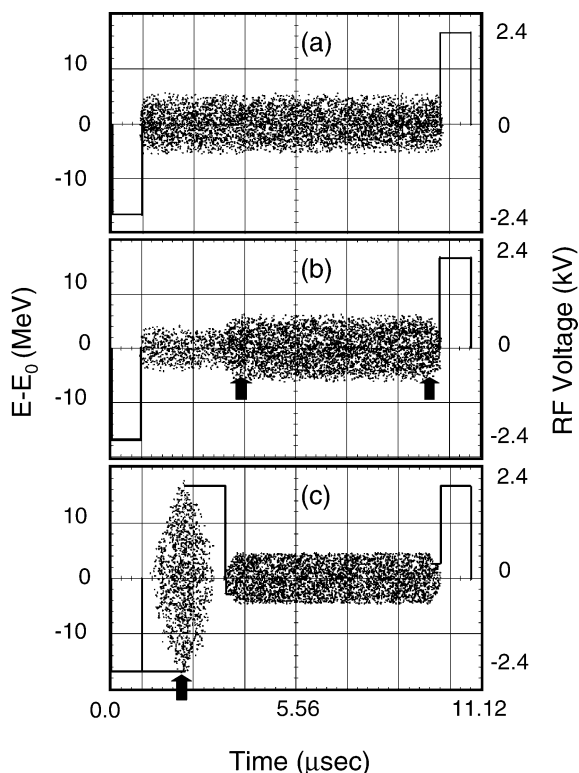


Fig. 2. Simulated barrier rf wave form (solid curve) and the  $(\Delta E, \tau)$  phase-space distribution of 100 eV s antiprotons in the Recycler for (a) initial beam distribution of length  $8.7 \mu\text{s}$ , (b) after populating the low longitudinal emittance particles to the right-hand side using  $-0.27$  kV rf pulse. The arrows indicate the final locations of the rf pulses used. In the simulation, the right side mining rf pulse ( $+0.27$  kV in height) was at a fixed position while the left rf pulse was clogged iso-adiabatically from left to right during shoveling in about 15 s. (c) After longitudinal momentum mining; the left bunch (indicated by an arrow) comprises of particles with high energy spread (bunch area  $\approx 51$  eV s) and the low longitudinal emittance particles are captured in the right-side bucket (bunch area = 54 eV s).

The simulation clearly showed that the amount of beam mined was a strong function of the energy distribution of particles. For a parabolic distribution, 74% of the beam was mined whereas for Gaussian distribution 64% was mined.

### 3.2. Beam studies

The beam tests were carried out using protons in the Recycler. About  $170 \times 10^{10}$  protons of longitudinal emittance  $110 \pm 15$  eV s (95% emittance) and energy

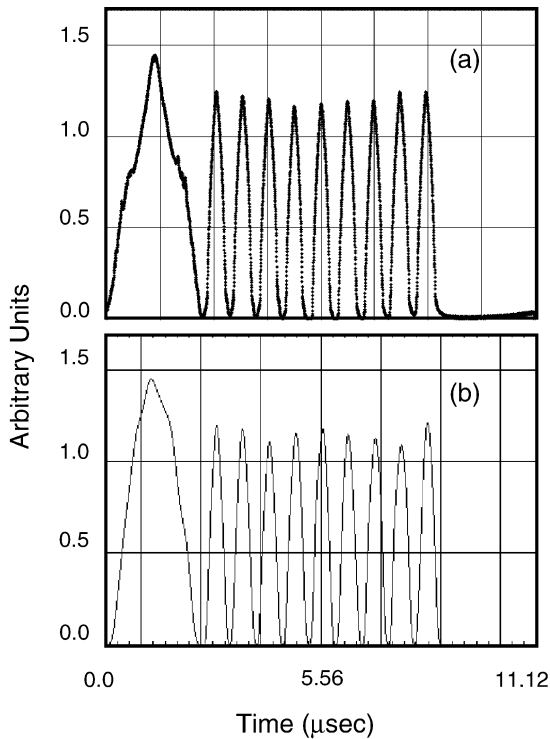


Fig. 3. (a) The measured and (b) predicted line-charge distribution for  $170 \times 10^{10}$  proton after longitudinal momentum mining and capturing high density low longitudinal emittance particles in the nine buckets and the rest in the left most bucket.

spread of  $\pm(14.3 \pm 0.6)$  MeV were stored in a  $3.7 \mu\text{s}$  wide rectangular barrier bucket of  $\pm 2$  kV pulse height. The beam was stretched slowly to  $8.7 \mu\text{s}$  and the momentum mining was performed essentially following the sequence studied in the simulation. Experimentally, the entire mining process took about 135 s while the simulation suggested about 110 s.

The wall current monitor data taken after the formation of nine bunches are shown in Fig. 3(a). The average longitudinal emittance of the beam in these nine buckets is  $5.6 \pm 0.6$  eV s (95% emittance) and the bunch on far left with particles of high energy spread has longitudinal emittance of  $55.5 \pm 12.5$  eV s (95% emittance). Fig. 3(b) is the corresponding simulated distribution. Experimentally, we find that about 65% of the beam particles are mined in the nine smaller buckets to be compared with 74% predicted by our simulation. The difference is due primarily to the difference between the energy distribution of the assumed ideal parabolic distribution for the ini-

tial energy spectrum, and the energy distribution of the un-cooled beam used for the experiments. We also see some qualitative difference between the shapes of the measured wall current monitor data (Fig. 3(a)) and the predictions (Fig. 3(b)). This difference is mainly attributed to (a) the initial energy distribution and (b) the details of rf pulse shapes used in the experiment and the one in the simulation (which was rectangular in shape).

#### 4. Remarks on issues at high beam intensities

The simulations presented here are carried out using single-particle beam dynamics in which we have not included beam space-charge or wake fields effects. Ordinarily, these effects must be taken in to account. However, for the case described above these effects are negligible. It is well known that at sufficiently high beam intensities the wake fields play an important role in the longitudinal beam dynamics and tend to disrupt detailed manipulations of phase space. In the case of the Fermilab Recycler, the average line-charge density during mining for the Tevatron transfers is expected to be about  $2 \times 10^{10}$  antiprotons/ $\mu\text{s}/\text{eV s}$  [16] at its design intensity. This is about a factor of four larger than the starting beam line-charge density used for the experimental demonstration of longitudinal momentum mining, in which no instability was seen. Furthermore, calculations for Recycler [12] including space-charge impedance and Landau damping indicate that the beam is stable even at  $1 \times 10^{13}$  antiprotons in the ring. Threshold impedance for microwave instability [19] for the Recycler is estimated to be about  $75 \Omega$ , which is smaller than the cavity impedances. If problem arises it can be suppressed with the standard cavity feedback techniques.

Recently, we have observed head-tail asymmetry in the longitudinal beam profiles for the stored beam in the Recycler in barrier rf buckets [20]. This asymmetry is understood in terms of the potential well distortion in the presence of the resistive impedance. We estimate that the baseline voltage inside the barrier bucket confining  $6 \times 10^{12}$  antiprotons will be reduced by about 100 V, which is just about 5% of the available peak rf voltage. Applying corrections to the barrier waves to counter this distortion is a trivial task.

## 5. Summary

I have proposed and validated a novel method for selectively isolating low longitudinal emittance particles and extracting them from a storage ring using rf barrier buckets. The scheme has been studied using multi-particle beam dynamics simulations and the technique has been demonstrated with beam experiments in the Recycler using protons. This method of momentum mining has been successfully implemented and is used routinely for beam extraction from the Fermilab Recycler. We have demonstrated the ability of this technique to extract antiproton bunches of constant longitudinal emittance and of constant intensity for multiple beam extraction from the Recycler with a variation  $\leq 10\%$  both for intensity and the longitudinal emittance from transfer to transfer. This feature of the longitudinal momentum mining is one of main advantages over the transverse momentum mining technique.

As a final note, I expect that the applications of the technique described here to selectively isolate the high density region of the phase space may not be unique to high-energy storage rings. This technique will be very useful for particle beam manipulation in future accelerators and it should have broad application in other low energy circular storage rings that use barrier rf systems.

## Acknowledgements

I would like to thank John Marriner, Pushpa Bhat, Jim MacLachlan and Harrison Prosper for many useful discussions during the course of this work. Thanks are also due to Brian Chase for his help on issues related to rf controls. My special thanks are due to Shreyas Bhat for a careful editing of the manuscript. I acknowledge the support of the US Department of Energy. Fermi National Accelerator Laboratory is operated by the Universities Research Association, under contract with the US Department of Energy.

## References

- [1] K.R. Symon, A.M. Sessler, in: Proceedings of the CERN Symposium on High Energy Accelerators, CERN, Geneva, 1956, p. 44.
- [2] J.E. Griffin, J.A. MacLachlan, Z.B. Qian, IEEE Trans. Nucl. Sci. 30 (4) (1983) 2627.
- [3] D.A. Edwards, M.J. Syphers, An Introduction to the Physics of High Energy Accelerators, first ed., John Wiley & Sons, New York, 1993.
- [4] Design Study of a Proton–Antiproton Colliding Beam Facility, CERN, Geneva, CERN/PS/AA 78-3 27.1.1978.
- [5] Design Report Tevatron 1 Project, Fermi National Accelerator Laboratory, Batavia, IL, Operated by Universities Research Association Incorporation, Under Contract with the US Department of Energy, September 1984. <http://library.fnal.gov/archive/design/fermilab-design-1984-01.shtml>.
- [6] S. Peggs, FERMILAB AP-Note-91-001, May 1991, unpublished, <http://library.fnal.gov/archive/apnote/fermilab-ap-note-91-001.shtml>.
- [7] W.E. Gabella, et al., in: Proceedings of the 1993 Particle Accelerator Conference, Washington DC, 1993, IEEE, Piscataway, NJ, 1993, p. 233.
- [8] C.M. Bhat, FERMILAB-FN-746, 2004, unpublished, <http://library.fnal.gov/archive/test-fn/0000/fermilab-fn-0746.shtml>.
- [9] G.E. Griffin, et al., IEEE Trans. Nucl. Sci. 30 (1983) 3502.
- [10] S.Y. Lee, K.Y. Ng, Phys. Rev. E 55 (1997) 5992.
- [11] S.Y. Lee, Accelerator Physics, first ed., World Scientific, Singapore, 1999, Chapter V, p. 305.
- [12] G. Jackson, Fermilab-TM-1991, November 1996, unpublished, <http://library.fnal.gov/archive/test-tm/1000/fermilab-tm-1991.shtml>.
- [13] J.E. Dey, D. Wildman, in: Proceedings of the 1999 Particle Accelerator Conference, New York, 1999, IEEE, Piscataway, NJ, 1999, p. 869.
- [14] D. Mohl, G. Petrucci, L. Thorndahl, S. van der Meer, Phys. Rep. 58 (1980) 75;  
D. Mohl, Advanced accelerator physics course, in: S. Turner (Ed.), Proceedings of the 1985 CERN Accelerator School, CERN 87-3 (1986) 453.
- [15] G.I. Budker, A.N. Skrinskii, Sov. Phys. Usp. 21 (1978) 277.
- [16] A. Burov, FERMILAB-CONF-03-171, unpublished, presented at International Workshop on Beam Cooling and Related Topics (COOL03), Japan, 19–23 May 2003, physics/0307053.
- [17] C.M. Bhat, in: W. Chou, et al. (Eds.), Proceedings of High Intensity and High Brightness Hadron Beam 20th ICFA Advance Beam Dynamics Workshop on High Intensity and High Brightness Hadron Beams, 2002, APS AIP Conf. Proc. 642 (2002) 229;  
C.M. Bhat, in: Proceedings of the 2003 Particle Accelerator Conference, Portland, OR, 2003, IEEE, Piscataway, NJ, 2003, p. 2345.
- [18] J.A. MacLachlan, in: International Conference on High Energy Accelerators, HEACC'98, Dubna, September 1998;  
J.A. MacLachlan, Fermilab report No. FN-529, 1989, unpublished, <http://www-ap.fnal.gov/ESME/>.
- [19] E. Keil, W. Schnell, CERN report TH-RF/69-48, 1969;  
V.K. Neil, A.M. Sessler, Rev. Sci. Instrum. 36 (1965) 469;  
D. Boussard, CERN report Lab II/RF/Int./75-2, 1975.
- [20] C.M. Bhat, K.Y. Ng, in: Factories 2003, Stanford, CA, 13–16 October 2003, FERMILAB-CONF-03-395-t, 2003, unpublished.